論文

PZT 및 PVDF 센서에 따른 음향방출과 Micromechanical 시험법을 이용한 단일 Basalt 섬유 강화 에폭시 복합재료의 비파괴 손상감지능 평가

김대식*, 박종만*+, 정진규*, 공진우**, 윤동진***

Evaluation of Nondestructive Damage Sensitivity on Single-Basalt Fiber/Epoxy Composites using Micromechanical Test and Acoustic Emission with PZT and PVDF Sensors

Dae-Sik Kim*, Joung-Man Park*+, Jin-Kyu Jung*, Jin-Woo Kong** and Dong-Jin Yoon***

ABSTRACT

Nondestructive damage sensitivity on single-basalt fiber/epoxy composites was evaluated by micromechanical technique and acoustic emission (AE). Piezoelectric lead-zirconate-titanate (PZT), polyvinylidene fluoride (PVDF) and poly(vinylidene fluoride-trifluoroethylene) (P(VDF-TrFE)) copolymer were used as AE sensor, respectively. In single-fiber composite, the damage sensing with different sensor types were compared to each other. Piezoelectric PVDF polymer sensor was embedded in and attached on the composite, whereas PZT sensor was only attached on the surface of specimen. In case of embedded polymer sensors, responding sensitivity was higher than that of the attached case. It can be due to full constraint inside specimen to transfer elastic wave coming from micro-deformation. For both the attached and the embedded cases, the sensitivity of P(VDF-TrFE) sensor was almost same as that of conventional PVDF sensor.

초 록

Micromechanical 시험법과 음향방출을 이용하여 단일 basalt 섬유 강화 에폭시 복합재료의 비파괴 손상감지능을 평가하였다. 음향방출 센서로는 세라믹 PZT 및 고분자 PVDF와 P(VDF-TrFE)를 사용하였고 단섬유 강화 시험법에서 각 센서 종류에 따른 손상감지능을 상호 비교하였다. 고분자 센서는 시편 표면에 부착시키거나 내부에 함침시켜 사용하였지만 PZT 센서는 표면에 부착하여 사용하였다. 고분자 센서를 시편 표면에 부착시킨 경우와 함침시킨 경우 감지능은 비슷하였지만 부착의 경우 debonding 신호가 많아 함침 시키는 방법이 손상감지에 더 효과적이었다. 손상 감지능은 PZT 센서가 가장 높았고, 함침 및 부착 모두에서 PVDF와 P(VDF-TrFE) 센서의 손상감지능은 거의 비슷하였다.

Key Words: 손상감지능(damage sensitivity), 비파괴적 평가(nondestructive evaluation), 미세역학시험법(micromechanical test), PVDF 센서(PVDF sensor), 음향방출(acoustic emission)

1. Introduction

Piezoelectric lead-zirconate-titanate (PZT) as a sensor has an

*+ 경상대학교 응용화학공학부 고분자공학전공, 항공기부품기술연구센터, 교신저자(E-mail:jmpark@nongae.gsnu.ac.kr)

* 경상대학교 응용화학공학부 고분자공학전공 대학원, 항공기부품기술연구센터

** 한국기계연구원 복합재료그룹

*** 한국표준과학연구원 스마트계측그룹

excellent sensitivity and a wide application of the structure materials, whereas PZT is brittle due to ceramic nature [1]. Recently, polymer film such as polyvinylidene fluoride (PVDF) and poly(vinylidene fluoride-trifluoroethylene) (P(VDF-TrFE)) copolymer have come into increasing use as a sensor [2,3].

Piezo film is a flexible, lightweight, tough engineering plastic available in a wide variety of thickness and large contacting area. Its properties as a transducer include: wide frequency range of 0.001 Hz to 9-10Hz, low acoustic impedance of close match to water, human tissue and adhesive systems, high elastic compliance and voltage output that is 10 times higher than *piezo* ceramics for the same force input, high dielectric strength, mechanical strength and impact resistance, and high stability on resisting moisture, most chemicals, oxidants, and intense ultraviolet and nuclear radiation [4,5]. Simple process and possible several shapes are also additional advantages. PVDF sensor can be directly attached or embedded to structure materials without disturbing its mechanical motion.

Acoustic emissions (AE) is well known as one of the important nondestructive evaluation (NDE) methods. AE is transient elastic wave generated by abrupt deformation within materials or structures [6,7]. AE can monitor the fracture behavior of composite materials, and can characterize many AE parameters to understand the type of microfailure sources during the fracture progressing. When tensile loading is applied to a composite, AE signal may occur from fiber fracture, matrix cracking, and sometimes debonding at the fiber-matrix interface [8,9].

In this study, nondestructive damage sensitivity for basalt fiber/epoxy composites was evaluated by PVDF and P(VDF-TrFE) copolymer sensors comparing to PZT sensor. Polymeric sensors were embedded in and attached on the epoxy matrix.

2. Experimental

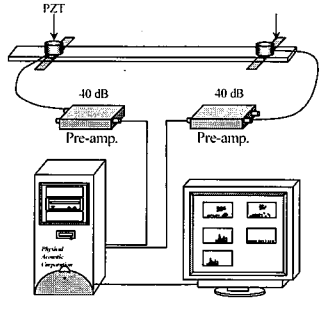

Fig. 1 Schematic diagram of AE system for source location and waveform analysis.

2.1 Materials

Used basalt fiber was made from naturally occurring basalt rock in the Washington State area. Virgin basalt fiber tensile strength can vary in the range 2-4 GPa depending on drawing conditions. Young's modulus and density were 85 GPa and 2.78 g/cm^3, respectively. The average diameter of the basalt fiber was about 97 ㎛.

Two types of PVDF and P(VDF-TrFE) copolymer films (Measurement Specialties Inc.) were used as piezoelectric polymer sensor. Piezoelectric properties are induced by high dielectric properties based on chemical structure. Semicrystalline PVDF and P(VDF-TrFE) copolymer exhibit the highest ferroelectric polarization and electro- mechanical responses among the known polymers.

Used epoxy resin (Kukdo Chemical Co. YD-128, Korea) is based on diglycidyl ether of bisphenol-A (DGEBA). Two types of polyoxypropylene diamine (Jeffamine D400 and D2000, Huntzman Pertochemical Co.) were used as curing agents. Flexibility of specimens was controlled by the relative proportions of D400 *versus* D2000.

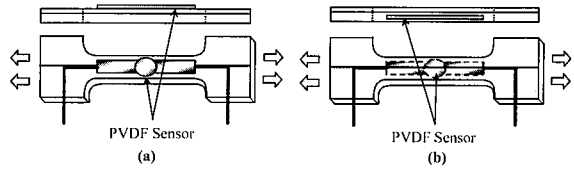

Fig. 2 Test specimen of single-fiber epoxy composite with (a) attached and (b) embedded polymer sensor.

2.2 Methodologies

2.2.1 Source Location and Waveform Analysis

Figure 1 shows the schematic diagram of AE system for source location and waveform analysis. Wave velocity of epoxy matrix was measured by two embedded PVDF sensors with 100 mm distance apart in one dimensional plate specimen. Beyond the interesting area of two sensors, AE sources were generated by pencil-lead-break method and thus the wave velocity of epoxy specimens were determined. The difference in the arriving time, Δt, was measured by using an in-built AE software. The wave velocity was calculated by the measurement of Δt, which is given as

$$\Delta t = \frac{D}{V} \tag{1}$$

where D is the distance between sensors, V is propagating velocity of an elastic wave. The critical location, d is given as

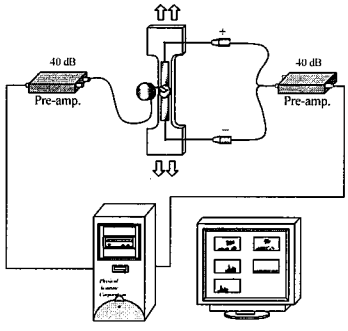

Fig. 3 Schematic AE system for damage sensing.

$$d = \frac{1}{2}(D - \Delta t V) \quad (2)$$

where d is the distance according to the first arriving sensor.

Waveform analysis of epoxy matrix was performed by PVDF and PZT sensors, and the result was compared to each other. The dimension of specimen was 100 mm in gauge length, 10 mm in width and 2 mm in thickness. The impacted damage sources were introduced at center and quarter between sensor 1 and sensor 2 by pencil-lead-break method.

2.2.2 Damage Sensing

AE signals were detected using a miniature PZT sensor (Resonance type, PICO by PAC) and two type polymeric sensors, i.e., PVDF and P(VDF-TrFE) copolymer. PZT sensor was attached on the surface of the specimen, whereas two polymeric sensors were embedded in and attached on the specimen to compare to the sensitivity as shown in Figure 2. PZT sensor has the peak sensitivity of 54 Ref V(m/s) and resonant frequency at 500 kHz. The outputs of two sensors were amplified by 40 dB at preamplifier gain. The threshold levels were set up as 30 dB for PZT sensor and as 35 dB for polymeric sensors, respectively. The threshold level of polymer sensor was set up rather higher than that of PZT sensor in order to delete the noise signals from polymer sensors. The signals were fed into an AE signal process unit (MISTRAS 2001) and AE parameters were analyzed using in-built software. Typical AE parameters such as hit rate, peak amplitude, and event duration were investigated for the time and the distribution analysis. Figure 3 shows schematic AE systems for the damage sensing.

3. Results and Discussion

3.1 Source Location and AE Waveform Analysis

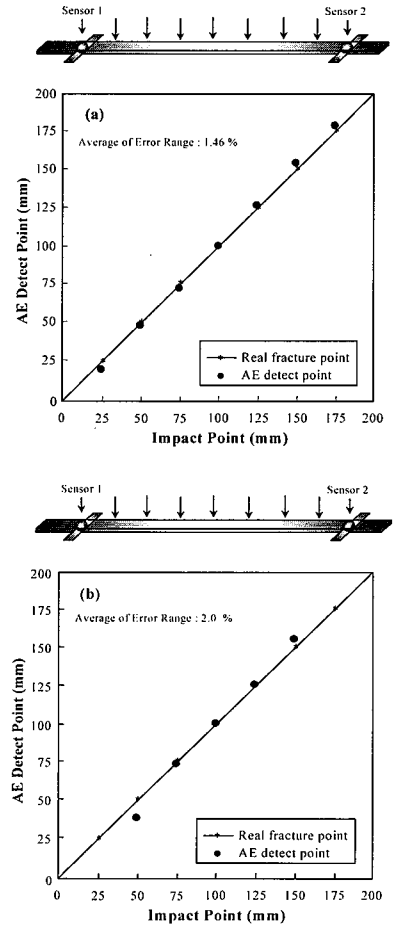

Fig. 4 Calibration curve for (a) Type A and (b) Type B, epoxy matrices with different toughness embedded with PVDF sensor.

Figure 4 shows the calibration curves for (a) Type A and (b) Type B, epoxy matrix controlled flexibility by PVDF sensor. Flexibility of epoxy matrix was controlled by the relative proportions of D400 *versus* D2000. Two-type epoxy matrices with different flexibility were chosen as follows: 3 g of D400 was used for Type A, whereas the used amount for D400 and D2000 was 2.5 g and 0.5 g for Type B, respectively. Generally the correspondence between impact points and AE detected points were established well for both type of cases. The flexibility and thus toughness of Type A was lower than that of Type B. Damping effect for elastic wave increased with increasing the toughness of polymer [10]. Figure 4(a) and (b) shows artificial damage which was induced by pencil-lead-break method with damage interval in 25 mm. In the PVDF case, the result of source location for Type A was matched well with real damage location, whereas the error range was larger

than that of PZT case as shown in the previous work [10]. For Type B, the error range was rather larger than Type A case. The damage far away from long distance could not be detected well due to low sensitivity of PVDF sensor and high damping effect due to the ductile polymer toughness.

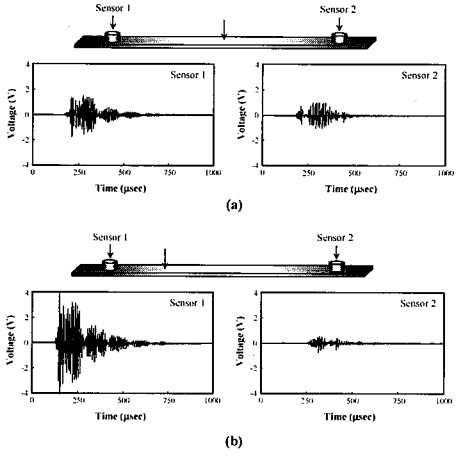

Fig. 5 AE waveform detected for (a) center impact and (b) quarter impact positions using two PZT sensors.

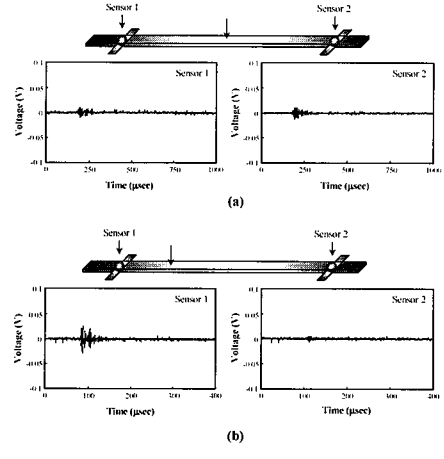

Fig. 6 AE waveform detected for (a) center impact and (b) quarter impact positions using two PVDF sensors.

Figures 5 and 6 show the AE waveform for (a) the centered impact and (b) quarter distanced impact detected by PZT and PVDF sensors, respectively. For centered impact case, wave voltages of sensor 1 and 2 were almost the same, whereas for quarter distanced impact the wave voltage of sensor 1 was higher than that of sensor 2 because the distance from damage source was shorter. Elastic wave is generally composed of two types of extensional and flexural waves in the case of plate type specimen. For quarter distanced impact position, waveform of sensor 1 was undistinguished from above three waveforms, whereas in the case of sensor 2 the extensional and flexural waves were distinguished well. It might be due to longer distance because the damage sources are well separated from each other. The velocity of extensional wave is known to be faster than that of flexural waves. The voltage of waveform detected by PVDF sensor was much lower than that of PZT sensor due to inherently lower responding properties of PVDF sensor. The trends of waveform for PVDF sensor with varying impact distance were similar to the results of PZT sensor, whereas above three elastic waves were not rather separated well as PZT sensor case. It can be said the damage sensitivity of PVDF sensor may be lower compared with PZT sensor from the results of source location and waveform analysis.

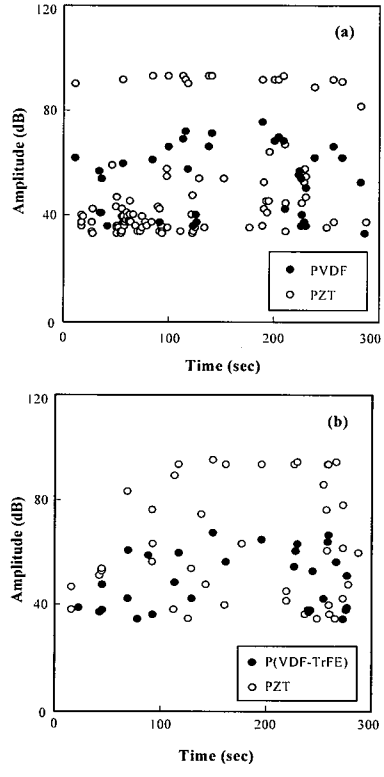

Fig. 7 AE amplitude of basalt fiber/epoxy composite detected by attached (a) PVDF and (b) P(VDF-TrFE) copolymer sensors.

3.2 Comparison of Damage Sensitivity with Sensor Types

Figures 7 shows the AE amplitude of basalt fiber/epoxy composite detected by attached with (a) PVDF and (b) P(VDF-TrFE) copolymer sensors. The objectives of this

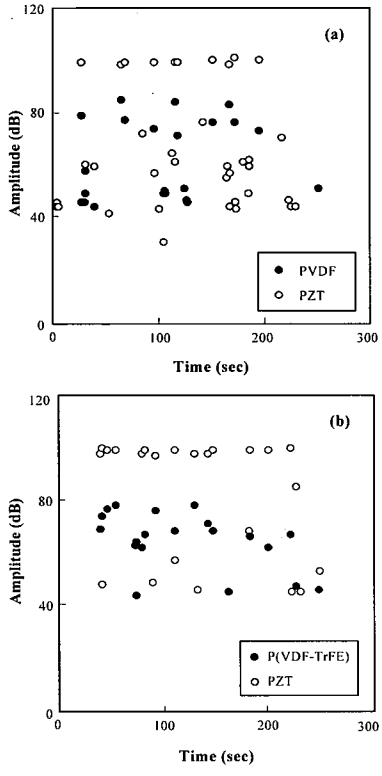

Fig. 8 AE amplitude of basalt fiber/epoxy composite detected by embedded (a) PVDF and (b) P(VDF-TrFE) copolymer sensors.

experiment were to know the effect of thicker fiber diameter and the different type of copolymer PVDF which is known to be stable thermally due to higher crystalline structure. Especially as an important additional experimental point, PVDF sensor was attached on the specimen's surface instead of embedded in the epoxy matrix. For both PVDF and P(VDF-TrFE) copolymer sensors, the number of AE signal was less than that of PZT sensor and AE amplitude was also much lower. Sensing of two piezoelectric PVDF sensors was almost the same for each other. For basalt fiber/epoxy system, matrix crack signals were detected as well as fiber fracture signals. AE signals below 40 dB were induced from matrix crack or debonding between surface of specimen and PVDF sensor. For both PVDF and P(VDF-TrFE) copolymer sensors, AE signals were detected until 300 seconds (about 8% strain) because they were embedded in the horizontal direction based on their higher sensitivity. This strain level might be still insufficient to be saturated for the consecutive breaking fiber fragment.

Figure 8 shows the AE amplitude of basalt fiber/epoxy composite detected by embedded (a) PVDF and (b) P(VDF-TrFE)

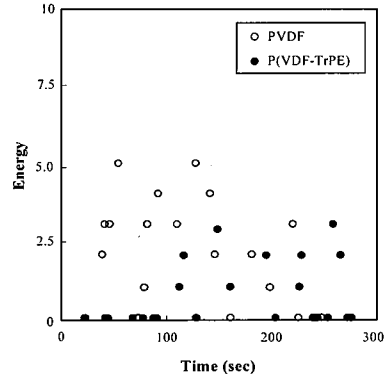

Fig. 9 AE energy of basalt fiber/epoxy composite detected by embedded PVDF and P(VDF-TrFE) copolymer sensors.

copolymer sensors. For both PVDF and P(VDF-TrFE) copolymer sensors, damage sensitivity was lower compared to PZT sensor like the attached case in Figure 7. Damage sensing of PVDF and P(VDF-TrFE) copolymer sensors was also similar to each other. In the embedded case, damage sensitivity was rather better compared to the attached case. It is because surface debonding signals between the surface of specimen and polymer sensor were detected rarely. In addition, the embedded surrounding contact area for sensing might contribute to the better sensing. Such unnecessary signals form surface detachment decreased the damage sensing.

Figure 9 shows the comparison of AE energy of basalt fiber/epoxy composite detected by embedded PVDF and P(VDF-TrFE) copolymer sensors. AE energy of PVDF sensor was higher compared to P(VDF-TrFE) copolymer sensor. However, it might be hard to say which sensor is more sensitive from AE energy results since the total number of AE event was similar to each other.

Figures 10 and 11 show the AE waveforms and their fast Fourier transform (FFT) for basalt fiber fracture in Figure 10 and matrix crack in Figure 11 detected by (a) PZT, (b) PVDF and (c) P(VDF-TrFE) copolymer sensors, respectively. For both fiber fracture and matrix crack signals, the voltage of waveform and frequency detected by PZT sensor were higher than those of PVDF sensors as expected. The voltage of fiber fracture was also much higher compared with matrix crack signal case. For basalt fiber, duration time was relatively shorter compared with glass fiber case. It may be related to short fracture duration time due to brittleness of thick basalt fiber compared to rather less brittle and thin glass fiber. Importantly matrix signals were detected clearly for both PVDF sensors from basalt fiber composites unlike glass fiber composite. It means that PVDF can also detect the matrix cracking as well as fiber break although the sensitivity is rather lower. The shorter duration time is, the lower AE energy is.

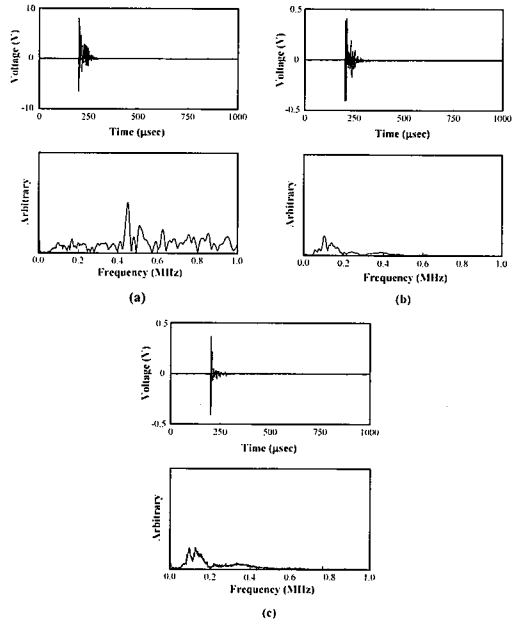

Fig. 10 AE waveforms and their FFT for basalt fiber fracture detected by (a) PZT, (b) PVDF and (c) P(VDF-TrFE) copolymer sensors.

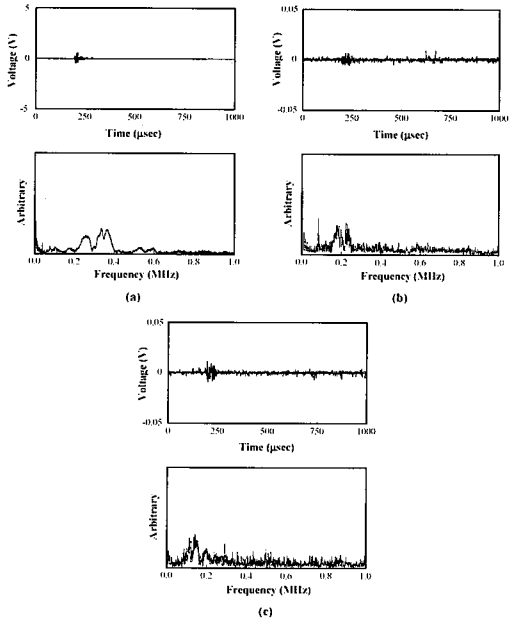

Fig. 11 AE waveforms and their FFT for epoxy matrix crack detected by (a) PZT, (b) PVDF and (c) P(VDF-TrFE) copolymer sensors.

4. Conclusions

Damage sensitivity on single fiber/epoxy composite with PZT and PVDF polymer sensors was evaluated by micromechanical test and AE. Damage sensitivity of PVDF and P(VDF-TrFE) copolymer sensors was similar to each other, whereas AE amplitude and AE energy for P(VDF-TrFE) copolymer sensor were lower compared to PVDF case. The damage sensitivity of two polymeric sensors was lower than that of PZT sensor from the results of source location and waveform analysis. In the embedded case, the damage sensitivity was rather higher than that of the attached case because surface debonding signals between specimen's surface and polymer sensor were detected rarely. PVDF sensor can be applicable to various composite materials by directly embedded or attached methods based on their flexibility without sensitivity loss.

Acknowledgment

This work was financially supported by National Research Laboratory (NRL) by Ministry of Science and Technology (MOST), Korea in Research Institute of Standards and Science (KRISS) through Research Center for Aircraft Parts Technology (ReCAPT), GNU, Korea.

References

1) Monkhouse, R.S.C., Wilcox, P.D., Cawley, P., "Flexible interdigital PVDF transducers for the generation of lamb waves in structures," *Ultrasonics* Vol. 35, 1997, pp. 489-498.

2) Bharti, V., Shanthi, G., Xu, H., Zhang, Q.M., Liang, K., "Evolution transitional behavior and structure of electron-irradiated poly(vinylidene fluoride-trifluoroethylene) copolymer films," *Materials Letter,* Vol. 47, 2001, pp. 107-111.

3) Tuzzolino, A.J., "Applications of PVDF dust sensor systems in space," *Advanced Space and Research,* Vol. 17, 1996, pp. 123-132.

4) Janiczek, T., "Analysis of PVDF transducer signals stimulated by mechanical tension," *Journal of Electrostatics,* Vol. 51-52, 2001, pp.167-172.

5) Teston, F., Chenu, C., Felix, N., Lethiecq, M., "Acoustelectric effect in piezocomposite sensors," *Material Science and Engineering C.* Vol. 21, 2000, pp. 177-181.

6) Bohse, J., "Acoustic emission characteristics of micro-failure processes in polymer blends and composites,"

Composites Science and Technology, Vol. 60, 2000, pp. 1213-1226.

7) Morscher, G.N., Gyekenyesi, A.L., "The velocity and attenuation of acoustic emission waves in SiC/SiC composites loaded in tension," *Composites Science and Technology,* Vol. 62, 2002, pp. 1171-1180.
8) Park, J.M., Kim, J.W., Yoon, D.J., "Interfacial evaluation and microfailure mechanisms of single carbon fiber/bismaleimide (BMI) composites by tensile and compressive fragmentation tests and acoustic emission," *Journal of Colloid and Interface Science,* Vol. 62, 2002, pp. 743-756.
9) Park, J.M., Kim, J.W., Yoon, D.J., "Comparison of interfacial properties of electrodeposited single carbon fiber/epoxy composites using tensile and compressive fragmentation tests and acoustic emission," *Journal of Colloid and Interface Science,* Vol. 247, 2002, pp. 231-245.
10) Park, J.M., Kong, J.W., Kim, J.W., Yoon, D.J., "Interfacial evaluation of electrodeposited single carbon fiber/epoxy composites by fiber fracture source location using fragmentation and acoustic emission," *Composites Science and Technology,* Vol. 64, 2004, pp. 983-998.